



Received Date : 16-Sep-2018

Revised Date : 26-Oct-2018

Accepted Date : 13-Nov-2018

Article type : Research Letter

**The flavonoid baicalin improves glucose metabolism by targeting the PH domain of
AKT and activating AKT/GSK3 β phosphorylation**

Shengnan Yang, Yuan Zhang, Fukui Shen, Xiaoyao Ma, Man Zhang, Yuanyuan Hou*, Gang Bai*

State Key Laboratory of Medicinal Chemical Biology, College of Pharmacy and Tianjin Key Laboratory of Molecular Drug Research, Nankai University, Tianjin, China

Correspondence: Yuanyuan Hou and Gang Bai

E-mail address: houyy@nankai.edu.cn and gangbai@nankai.edu.cn.

Abbreviations:

AKT: PKB (protein kinase B)

GSK3 β : glycogen synthase kinase 3 β

PH domain: pleckstrin homology domain

PIP3: PtdIns(3,4,5)P3

This article has been accepted for publication and undergone full peer review but has not been through the copyediting, typesetting, pagination and proofreading process, which may lead to differences between this version and the Version of Record. Please cite this article as doi: 10.1002/1873-3468.13305

This article is protected by copyright. All rights reserved.

Accepted Article

PIP2: PtdIns(3,4)P2

BDP: boron dipyrromethene fluorophore

Met: metformin Hydrochloride

MMs: magnetic microspheres

Sulfo-SADP: [sodium 1-((3-((4-azidophenyl) disulfanyl) propanoyl) oxy)-2,5-dioxopyrrolidine-3-sulfonate]

DTT: DL-dithiothreitol

FSA: fluorescent-labeled anti-rabbit IgG secondary antibodies

LiCl: Lithium Chloride Anhydrous

Abstract

Baicalin is one of the main flavonoids of the dried root of *Scutellaria baicalensis* Georgi and is reported to exert beneficial effects on the regulation of glucose/lipid metabolism. However, understanding its specific target and unique mechanism for improving glucose utilization is a challenge. In this paper, target fishing with a baicalin probe reveals that baicalin interacts with AKT. An immunofluorescence assay further demonstrates the colocalization of baicalin with AKT in the cytoplasm. A competitive test and virtual docking show that baicalin might bind to the pleckstrin homology (PH) domain of AKT. This specific binding hampers AKT membrane translocation, activates the phosphorylation of AKT on Ser473, induces the downstream glycogen synthase kinase 3 β (GSK3 β) activation, and affects glycogen synthesis.

Keywords: baicalin; glucose metabolism; AKT; PH domain; GSK3 β

Introduction

Diabetes is a chronic metabolic disorder in which blood glucose levels are abnormally elevated (hyperglycemia) [1], and it has long been a major disease that harms human health [2]. Insulin resistance results in damage to the tissues of the liver, muscles, fat and other tissues involved in the regulation of blood glucose metabolism and plays a key role in type 2 diabetes (T2D) [3-5]. For a long time, the link between insulin resistance, obesity and T2D has been investigated [6].

AKT, also known as PKB (protein kinase B), is a Ser/Thr kinase, is an important node protein of the insulin signaling pathway and the phosphatidylinositol 3-kinase (PI3K) signaling pathway. AKT is mainly expressed in insulin-responsive tissues involved in the regulation of glucose homeostasis [7,8]. The modular structure of AKT consists of a C-terminal regulatory domain, an N-terminal pleckstrin homology (PH) domain and a kinase catalytic domain in the middle [7-9]. The products of PI3K activation, PIP3 and its immediate decomposition product PIP2, both trigger physiological processes by interacting with proteins having a PH domain [10]. One of the characterized PIP3/PIP2 effector proteins is the AKT protein [11]. AKT plays a pivotal role in insulin resistance [12,13], and the relationship between the suppression of the PI3K-AKT signaling pathway and diabetes is mostly concentrated [14,15]. The PI3K-AKT signaling pathway regulates the expression of gluconeogenesis genes and fatty acid synthesis genes by regulating the activity of downstream molecules, such as forkhead box protein O1 (FOXO1) and GSK3 β . Hence, the activation of AKT is the integral result of multiple inputs to regulate glucose utilization and lipid metabolism [6].

Baicalin is one of the most valid and abundant flavonoid component extracts in the roots of *Scutellaria baicalensis*, with antidiabetic and neuro-protective activities and anti-inflammatory and antidyslipidemic properties [16-19]. In a previous report, Guo et al found that baicalin inhibited p38 and NF- κ B phosphorylation to suppress the pro-inflammatory cytokines IL- β , IL-6, and TNF- α [20]. In addition, Fang et al found that baicalin activated the AKT/AS160/GLUT4 pathway to combat against obesity and insulin resistance [21]. Recently, chemo proteomics research reveals that baicalin ameliorates

obesity and hepatic steatosis by activating hepatic CPT1 [22]. Furthermore, it is reported that baicalin possesses the ability to prevent skeletal muscle ectopic fat storage and insulin resistance by regulating the AKT/GSK3 β pathway [23]. Although the benefits of baicalin in the regulation of glucose metabolism has been confirmed, the underlying target and mechanism of the hypoglycemic effect of baicalin are not clear yet.

In this study, we tried to identify the targets of baicalin by integrated chemical biology methods. For clarifying the key target protein on insulin resistance pathways, a novel alkynyl-modified baicalin probe was synthesized and used for target capture and cell localization in HepG-2 cells. A set of ligand competitive tests and virtual docking experiments were utilized to obtain a binding pocket of the target protein. After a membrane transport test and downstream signaling pathway evaluation, the potential molecular mechanism of how baicalin improves glucose metabolism through the insulin and PI3K/AKT signaling pathways was revealed.

Materials and Methods

Reagents

Baicalin and baicalein were acquired from the Shanghai Yuan Ye Biotechnology Company Ltd. (Shanghai, China, purity 98%). BDP TMR azide was purchased from Aladdin (Shanghai, China). Metformin Hydrochloride (Met) was from Adams Reagent, Ltd. (Shanghai, China). Sodium 1-((3-((4-azidophenyl) disulfanyl) propanoyl) oxy) -2,5-dioxopyrrolidine-3-sulfonate (Sulfo-SADP) was obtained from Bioworld (MN, USA). Fe₃O₄ amino magnetic microspheres (NH₂-MMs) was purchased from Tianjin baseline Chromtech Research Center (Tianjin, China). The plasmids pcDNA3-AKTPH-GFP (Addgene ID: 18836) and pcDNA3-AKTPH(R25C)-GFP (Addgene ID: 18837) were obtained from Addgene (MA, USA). Lipofectamine 2000 was purchased from Invitrogen (Carlsbad, CA, USA). The enzyme activity assay kit of AKT and GSK-3 β were purchased from GenMed Scientific Inc. (Arlington, MA, USA). Primary antibodies, including PDK1, p-PDK1, AKT, p-AKT (Thr308 or Ser 473),

GSK-3 β , p-GSK-3 β , and GAPDH, and the secondary antibody were obtained from Cell Signaling Technology (Beverly, MA, USA). The chemiluminescent HRP substrate was purchased from the Millipore Corporation (MA, USA). The glucose assay kit was obtained from Nanjing Jiancheng Biological Technology Co. Ltd. (Nanjing, China). The fluorescent-labeled anti-rabbit IgG secondary antibodies (FSA; Alexa Fluor[®] 594) were obtained from Abcam (Cambridge, UK). SC79 and AKT inhibitor VIII were purchased from MCE (NJ 08852, USA). PHT-427 and AT7867 were from Selleck (Shanghai, China). All the cell culture reagents were purchased from GibcoBRL Life Technologies (Grand Island, NY, USA). All the other chemicals used were of analytical grade.

Cell culture

Human hepatoma HepG-2 cells were cultured in DMEM, containing 10% fetal bovine serum, streptomycin (100 mg/mL) and penicillin (100 U/mL) [24]. The HEK293 stable cell line, derived from human renal epithelial cells, were also cultured in DMEM with 10% fetal bovine serum, 100 U/mL penicillin and 100 mg/mL streptomycin. All the cells were maintained in a 5% CO₂ humidified atmosphere at 37°C. All the cell culture reagents were purchased from American Type Culture Collection (Rockville, MD)

Synthesis of the alkynyl-modified baicalin probe

Di-succinimidyl carbonate (688 mg, 2.688 mM) was added to a solution of baicalin (400 mg, 0.896 mM) and pyridine (0.433 ml, 5.376 mM) in 25 ml of dichloromethane, and it was stirred overnight at room temperature. After completion of the reaction, 50 mL of dichloromethane was added for extraction, and the organic layer was washed with 20 mL of HCl (1 M), 20 mL of NaHCO₃ (saturation), and 20 mL of saturated brine, in that order, and then, the organic layer was collected as a yellow solid, which was the crude intermediate. This crude product and N,N-Diisopropylethylamine (DIEA) (178 μ L, 1.075 mM) were dissolved in 20 mL of N,N-Dimethylformamide (DMF), and propargylamine (59.2 μ L, 1.075 mM) was added slowly

under ice-cooling and was slowly warmed to room temperature under argon protection overnight, as shown in Figure S1. To obtain an alkynyl-modified baicalin probe (yellow solid), the mixture was centralized in vacuo and was purified by column chromatography on a silica gel (dichloromethane: methanol=10:1). The yield of this reaction was 67% (290 mg). In the supporting information, the detailed NMR data are included ((Figure S2) and the (-)-HR-ESI-MS spectrum of alkynyl-baicalin is shown in Figure S3).

Target prediction of baicalin

To predict the protein target of baicalin, a pharmacophore matching platform PharmMapper (<http://59.78.96.61/pharmmapper/>) was utilized. The 3-dimensional structure of baicalin, generalized by Chemdraw professional 15.0, was submitted to PharmMapper for target prediction. The protein interactions were analyzed using String10.5 (<http://www.string-db.org/>), and the pathways were excavated using the KEGG PATHWAY Database (<https://www.genome.jp/kegg/pathway.html>). The three-dimensional structures of the AKT-PH domain (PDB: 1H10) was obtained from the Protein Data Bank (<http://www.rcsb.org>). To illustrate the interaction between baicalin and target proteins, Molecular Operating Environment 2015.10 (MOE) and AutoDock version 4.2 (Olson Laboratory, LaJolla, CA) docking software were applied for docking, and SYBYL (Chemical Computing Group, Inc.) was used to construct the structure of baicalin and the potential protein targets and to minimize their energy.

Target fishing

HepG-2 cells were cultured with DMEM complete medium for 24 h in 75 cm² culture flasks. Subsequently, the cells were washed with a precooled PBS solution 3 times, and 0.5 mL of RIPA lysis buffer (China COSCO, Beijing, China) was added for 30 min on ice followed by collection with a cell scraper. Then, the lysate (at 4°C) was centrifuged at 12,000 rpm for 10 minutes. The lysate was centrifuged (12,000 rpm) for 10 min at 4°C, and the BCA protein

assay kit (Thermo Scientific, Waltham, MA, USA) was used to quantify the supernatant. The protein concentration was adjusted to 1 mg/ml in precooled hypotonic buffer. After that, the baicalin-modified functionalized MMs (See support information Figure S4 and Figure S5 for details.) were added. The mixture was incubated at 4°C with gentle shaking overnight. After collecting by magnetic separation, the MMs were rinsed with precooled PBST 3 times. The proteins bound by baicalin were released by an incubation with 200 μ L the DTT (100 mM) for 30 min at 4°C, and the supernatants were gathered for SDS-PAGE and the western blot analysis.

Colocalization in cells

HepG-2 cells were cultured at a suitable density in glass bottom dishes, and they were treated with or without an alkynyl-modified baicalin probe (10 μ M) for 6 h when the cells reached approximately 60% confluence. After washing, the treated cells were fixed in 4% paraformaldehyde for 15 min and then they were washed with PBST 3 times. Next, the cells were blocked with 5% goat serum for 1 h and were incubated with an anti-AKT antibody (1:200) at 4°C overnight. Then, they were treated with fluorescent-labeled anti-rabbit IgG secondary antibodies (FSA; Alexa Fluor[®] 594) for 1 h at 37°C. After washing with PBST 3 times, the fixed cells were taken through the biorthogonal click reaction with 100 μ L of BDP reaction solution (10 μ M BDP TMR azide, 20 μ M Tris-triazoleamine, 10 μ M CuSO₄, and 20 μ M sodium ascorbate) at room temperature for 1 h. After an adequate number of washes, the fluorescence images were obtained with a confocal microscope (Leica TCS SP8, Japan). The excitation and emission wavelengths for FSA (Alexa Fluor[®] 594) were employed at 594 nm and 617 nm and for BDP TMR azide they were employed at 514 nm and 570 nm, respectively.

SDS-PAGE and western blot analysis

SDS-PAGE (10%) was conducted using a general protocol. Briefly, the cells were washed with precooled PBS two times and were lysed with RIPA lysis buffer for 30 min on ice. The cell lysates were centrifuged at 12000rpm for 15 min at 4°C to obtain the supernatants. The supernatants or the captured protein were mixed with loading buffer, were boiled and were loaded for SDS-PAGE and Coomassie Blue staining if necessary. The other SDS-PAGE gel was transferred to a PVDF membrane for a western blot analysis. After transfer, the membrane was blocked with 5% skim milk for 1 h and was incubated with a primary antibody (1:1000) overnight at 4°C. After rinsing with PBST, the membrane was then incubated with a secondary antibody (1:2500) at room temperature for 1 h. After adequate washing, the membranes were incubated with chemiluminescent HRP substrates and were exposed in a Tanon-5200 Chemiluminescence Apparatus (Shanghai, China). The relative optical densities of the bands were quantified using the free software ImageJ.

Competitive test

The fresh mouse liver was homogenized and was placed in RIPA lysis buffer at a rate of 1 g/ml and was gently ground and lysed on ice for 30 min. Then, the lysate was centrifuged (12,000 rpm) for 10 min at 4°C. The target protein capture process by the baicalin-modified functionalized MMs was the same as the above target fishing process, except the last protein release step. As a positive control group, the enriched proteins were released with 200 μ L of DTT, just as described in the above section. In the competition groups, the captured AKT proteins were competed with 200 μ L of different 10 μ M competitors (SC79, AKT inhibitor VIII, AT7876 and PHT-427) at 4°C for 30 min. Similarly, the released proteins in the supernatants were collected for AKT detection by a western blot.

AKT plasma translocation assay

To detect the AKT translocation effects, the HEK293 transiently transfected cell lines expressing the AKT^{PH}-GFP or AKT^{PH}(R25C)-GFP fusion proteins were generated. The HEK293 cells were plated in a glass bottom dish for 24 h. Subsequently, transfection of the two plasmids was performed separately (the ratio of the PEI to plasmid mass was 6:1), and the transfection time was 6 h. Prior to transfection, the cells were incubated with DMEM cultures that solubilized SC79, baicalin or baicalein to prevent the overexpression of the AKT-PH-GFP membrane translocation. Subsequently, the GFP images were captured with a spectral-type AF7000 Live Cell Imaging System (Carl Zeiss, Oberkochen, Germany). The excitation and emission wavelengths of GFP were set as 488 nm and 507 nm, respectively.

Enzymatic activity assay

HepG-2 cells were plated in 75 cm² culture flasks and were cultured with DMEM complete medium for 24 h. Then, the cell lysates were prepared as described in the above section. Afterwards, the lysates were divided into several equal parts of 100 µl each. They were the control group, baicalin group (0.1, 1 and 10 µM) and positive drug group, which included SC79 (10 µM) as an agonist of the AKT enzyme activity and LiCl (10 µM) as an inhibitor of GSK3β enzyme activity. After synchronization, each group was bathed in a 37°C water bath for 45 min. Then, the enzymatic activities of the AKT and GSK3β in cell lysates were quantified as described in the manufacturer's manual (GENMED, Arlington, MA, USA).

Glucose consumption assay

HepG-2 cells were grown in 96-well culture plates at a density of 2×10⁴ cells per well. After 24 h incubation, the culture medium was replaced by the serum-free medium with or without 1 µM insulin for the next 24 h. Then, the cells in the different treatment groups were treated with baicalin or Met (10 µM) for another 12 h. Then, the supernatants were collected for the glucose concentration assay using the glucose assay kit (Nanjing Jiancheng Bioengineering

Institute, Nanjing, China) based on glucose oxidase method, according to the manufacturer's instructions.

Statistical analysis

The results are reported as the means \pm SD (standard deviations). The statistical analysis was performed using Prism 5.01. For single comparisons, significant differences between the means were determined using a Student's t test. The significance was accepted as $P < 0.05$.

Results and Discussion

Identification of AKT as a target of baicalin

To capture the target protein of baicalin from the cells, an alkynyl-modified baicalin probe was synthesized as a tracer. Then, the baicalin-modified functionalized MMs were prepared by a click reaction in vitro, according to the scheme shown in Fig. 1A. Next, the functionalized MMs were used to capture the protein target in the HepG-2 cells, and the disulfide bond between the MMs and baicalin probe was broken by DTT to release the captured proteins. To identify the target proteins of baicalin, SDS-PAGE and Coomassie brilliant blue staining were performed to evaluate the collecting efficiency. As shown in the left panel of Fig. 1B, the total protein in the HepG-2 cell lysate is detected and is shown as lane 1. Compared to the negative control group in lane 2 (only azide-modified MMs), the functionalized MMs enriched proteins from the cell lysate are shown in lane 3. This result indicated that these enriched proteins were selective for the baicalin probe.

For identifying the target proteins, PharmMapper was carried out to predict the potential target proteins of baicalin based on its 3D structure. The top 30 target proteins (based on the fit value) screened were listed in Table S1. The String10.5 analysis was performed to determine the inner linkage among the selected proteins. As shown in Fig. 1C, the top five pathways (based on the q value) were the insulin signaling pathway (red), the

PI3K-AKT signaling pathway (blue), the prolactin signaling pathway (yellow), prostate cancer (green) and the Rap1 signaling pathway (purple) (Table S2). Analyzing these pathways suggested that the insulin signaling pathway[25] and the PI3K-AKT signaling pathway [26] were the most related to glucose and lipid metabolism. In addition, previous reports of baicalin-regulated glucose metabolism and insulin resistance mainly focus at these two signaling pathways [21,27].

By analyzing the relationship between the five pathways, AKT1 and HRAS were the most important nodes and were speculated as two potential targets of baicalin. To confirm the hypothesis, we performed a western blot validation via the captured proteins. The same SDS-PAGE gel was transferred to a PVDF membranes for the western blot analysis. As shown in Fig. 1B on the right, the total protein from the HepG-2 lysate, shown in Lane 1, detected AKT1 and HRAS. Compared with Lane 1, the lysate enriched by the baicalin-modified MMs was defined as Lane 3, and AKT was accurately captured while Ras was not. Based on this result, we speculated that AKT may be one of the key targets of baicalin in regulating glucose metabolism.

Colocalization with AKT in the cells

To explore the interaction between baicalin and AKT, the click reaction between the BDP TMR azide fluorochrome and the baicalin probe was carried out (Fig. 2A). As shown in Fig. 2B, the conjugate ring in the click product shows a strong green fluorescence that is clearly observed in the cytoplasm, and the red fluorescence of FSA (Alexa Fluor[®] 594) reflects the distribution of AKT. The untreated baicalin probe showed little fluorescence in the control group. The distribution of AKT (red) was also observed in the cytoplasm and partially merged (yellow) with the baicalin probe. These results suggested that AKT proteins might be the target of baicalin under cellular conditions.

Baicalin binds to the PH domain of AKT

As mentioned, the modular structure of AKT consists of the PH domain, the kinase catalytic domain and the regulatory domain [8]. To verify the binding pocket of AKT with baicalin, we designed a competition experiment. A set of AKT ligands (SC79, PHT-427, AKT VIII and AT7876) were chosen to compete with AKT, which were captured by the baicalin-modified functionalized MMs. SC79 is a specific AKT-PH domain inhibitor that targets the PH domain of AKT, which in turn activates AKT [28]. PHT427, a novel Akt/phosphatidylinositol-dependent protein kinase 1 PH domain inhibitor, inhibits the activity of AKT [29]. AT7867 is an ATP-competitive inhibitor, which competes with ATP at the ATP binding site and inhibits the activity of AKT [30]. AKT VIII is reported as an allosteric inhibitor of AKT kinase, which will also restricts the activity of AKT [31]. As shown in Fig. 3A, the results showed that both the agonist (SC79) and antagonist (PHT-427) of the PH binding domain of AKT specifically competed with the baicalin-bound probe, which was similar to the positive group that released AKT after DTT reduction. This result indicated that baicalin might combine with the AKT-PH domain.

As a natural ligand of the AKT-PH domain, PIP3 binds to the PH domain of AKT in a shallow pocket. It is then mediated by several salt bridges between the phosphate groups and basic residues in the protein [28]. 4IP is a known ligand for the AKT-PH domain, and it lacks only long-chain hydrocarbons for the membrane hang compared to PIP3. It is known that the activation of PI3K converts PIP2 to PIP3, instead of PIP2 binding to the AKT-PH domain, and the hydrogen bond interactions at Lys14, Arg25 and Arg86 of the AKT-PH are regarded as the key amino residues, which are closely related to membrane translocation [32]. In addition, the other amino acid residues, such as Arg23 and Asn53, are also reported to be important. The interaction of Arg23 with the D1 phosphate plays a role in regulating the overall affinity of AKT for 3-phosphoinositides. Additionally, a slight reduction in the binding is observed for the Asn53 mutation (which interacts with the D3 and D4 phosphates). As shown in Fig. 3B, the molecular docking of MOE for the AKT-PH domain demonstrated that SC79, baicalin and 4IP bound with the key amino acid Asn53 (N53) and Arg25 (R25). A previous study showed that Arg25 in the AKT PH domain sequence is essential for AKT's binding

ability with 4IP (third carbon atom at inositol). If Arg25 is inhibited or mutated, AKT cannot be translocated to the plasma membrane [32].

It is reported that AKT translocation to the plasma membrane promotes its phosphorylation to sustain AKT activity [33]. To investigate whether baicalin has the same effect on the direct activation of AKT as SC79, GFP tagged AKT-PH domains were used to follow the subcellular localization of AKT in HEK293 cell lines. After transfecting with the respective plasmids for 6 h, two kinds of fusion proteins, namely, AKT^{PH}-GFP and AKT^{PH(R25C)}-GFP, were generated. Among these, AKT^{PH(R25C)}-GFP was a positive control because its AKT-PH-GFP protein cannot be translocated to the membrane under the stimulation of insulin-like growth factor 1 (IGF1) [31]. The expressed AKT^{PH}-GFP fusion protein was a tracer that was used to detect and evaluate the AKT plasma membrane translocation phenomenon.

After transfection, IGF-1 (10 μ M) was used to stimulate the cells for 10 min, and the induction of AKT-PH membrane translocation occurred. Compared with the IGF-1- induced AKT-PH membrane translocation effect in the AKT^{PH}-GFP-HEK 293 cells, baicalin inhibited the occurrence of AKT-PH's translocation to the membrane in a dose-dependent manner, just as SC79 did (Fig. 3C)

Baicalein is an aglycone metabolized form baicalin. Once absorbed into the body, baicalein undergoes extensive first-pass glucuronidation to glucuronide conjugates, such as baicalin, in both the liver and intestine [34,35]. Molecular docking showed that the carboxy group from the D-glucuronic acid of baicalin, which bound with Arg25 and Arg23 (Fig. 3B), occupied the PIP3 binding active pockets near the Arg25, inhibited the interaction between the phosphoryl group of PIP3 and Arg25, and reduced the transmembrane activity of AKT (Fig. 3C). When baicalein lost the D-glucuronic acid from the baicalin, it did not impact the transmembrane function of AKT (Fig. 3C).

Baicalin promoted glucose consumption by inducing the phosphorylation of AKT and GSK3B

The activation of AKT enhances glycogen synthesis via the direct phosphorylation and inhibition of GSK3 [36]. Phosphorylated GSK3 β activates a number of intracellular signaling pathways, including glucose metabolism, the regulation of cell differentiation and cell survival [37,38]. The increased phosphorylation of GSK-3 β protein also contributes to insulin resistance by affecting glycogen synthesis [39].

To evaluate the effect of baicalin on AKT activation, the upstream and downstream protein expression levels of AKT in the PDK1/AKT/GSK3 β axis were examined after baicalin charging 1 hour. As shown in Fig. 4A, baicalin does not change the phosphorylation level of PDK1, but the amount of AKT phosphoprotein (only in Ser473 not Thr308) is upregulated in a dose-dependent manner. For the downstream proteins, baicalin also upregulated the phosphorylation of GSK-3 β . Further exploration of the enzyme activity testified that baicalin increased the enzyme activity of AKT and deactivated GSK3 β , as shown in Fig. 4B and C. Activated AKT phosphorylated and deactivated GSK-3 β , leading to the activation of glycogen synthesis and downregulating the blood glucose level (Fig. 4D).

Baicalin-induced AKT activation

The activation of AKT, by the regulation of phosphorylation, is caused by the PIP3-mediated plasma membrane translocation. It is reported that PIP3 not only phosphorylates AKT but also induces conformational changes in AKT, promoting AKT phosphorylation [28,40-42]. The AKT1/2 isoforms contain two regulatory phosphorylation sites at Ser473 in the C-terminal of the kinase domain (EXT domain) and Thr308 in the activation loop (CAT domain) [43]. Normally, the conformational change of AKT exposes the phosphorylation sites and promote the phosphorylation and activation of AKT, and at the same time, it is demonstrated that chemically induced cytoplasmic AKT allosteric activation bypasses the need for AKT membrane recruitment [28].

The deactivation of AKT contributes insulin resistance in type 1 and 2 diabetes. Under these pathological conditions, elevating AKT activity becomes an obvious clinical strategy for inhibiting insulin resistance [28]. In the absence of PIP3, AKT is in the off-inactivated state, and the binding of PIP3 to the PH domain makes it a more favorable conformation to release this intramolecular constraint. The baicalin-induced AKT conformation change that is favorable for the phosphorylation site at Ser473 may act similarly to PIP3. It activates AKT in the cytosol and bypasses the PIP3-mediated AKT membrane translocation requirements (Fig. 5).

In conclusion, our research suggested that baicalin enhanced glucose metabolism by targeting the critical activation site of the AKT-PH domain. Although AKT membrane translocation is hampered, its phosphorylation at S473 activates downstream proteins, such as GSK3 β , contributing to insulin resistance via affecting glycogen synthesis. The approach presented in this paper suggests that directly activating the AKT-PH PIP3 binding pocket may have considerable potential in the regulation of metabolic diseases, and also provides insights for the development of AKT agonists for treating insulin resistance.

References

- [1] George, G., Joseph, J. and Ganjifrockwalaa, F. (2017). Decreased total antioxidant levels and increased oxidative stress in South African type 2 diabetes mellitus patients. *JEMDSA* 22, 21-25.
- [2] Ugwu, T.E. and Ikem, R.T. (2017). Performance of the Androgen Deficiency in Aging Male questionnaire for the clinical detection of androgen deficiency in black sub-Saharan African men with Type-2 diabetes mellitus. *JEMDSA* 22, 60-63.
- [3] Conte, C., Epstein, S. and Napoli, N. (2018). Insulin resistance and bone: a biological partnership. *Acta Diabetol* 55, 305-314.
- [4] Wang, S. S., Li, Y. Q., Liang, Y. Z., Dong, J., He, Y., Zhang, L. and Yan, Y. X. (2017). Expression of miR-18a and miR-34c in circulating monocytes associated with vulnerability to type 2 diabetes mellitus and insulin resistance. *J. Cell. Mol. Med.* 21, 3372-3380.
- [5] Joatar, F. E., Al Qarni, A. A., Ali, M. E., Al Masaud, A., Shire, A. M., Das, N., Gumaa, K. and Giha, H. A. (2017). Leu72Met and Other Intronic Polymorphisms in the GHRL and GHSR Genes Are Not Associated with Type 2 Diabetes Mellitus, Insulin Resistance, or Serum Ghrelin Levels in a Saudi Population. *Endocrinol Metab* 32, 360-369.
- [6] Samuel, V. T. and Shulman, G. I. (2016). The pathogenesis of insulin resistance: integrating signaling pathways and substrate flux. *J Clin Invest* 126, 12-22.
- [7] Manning, B. D. and Toker, A. (2017). AKT/PKB Signaling: Navigating the Network. *Cell* 169, 381-405.
- [8] Brazil, D. P., Park, J. and Hemmings, B. A. (2002). PKB binding proteins. Getting in on the Akt. *Cell* 111, 293-303.
- [9] Satoh, N., Nakamura, M., Suzuki, M., Suzuki, A., Seki, G. and Horita, S. (2015). Roles of Akt and SGK1 in the Regulation of Renal Tubular Transport. *Biomed Res Int* 2015, 971697.
- [10] Milburn, C. C., Deak, M., Kelly, S. M., Price, N. C., Alessi, D. R. and Van Aalten, D. M. (2003). Binding of phosphatidylinositol 3,4,5-trisphosphate to the pleckstrin homology domain of protein kinase B induces a conformational change. *Biochem J* 375, 531-8.
- [11] Bago, R. et al. (2016). The hVps34-SGK3 pathway alleviates sustained PI3K/Akt inhibition by stimulating mTORC1 and tumour growth. *Embo Journal* 35, 1902-1922.

- Accepted Article
- [12] Xian, H.-m., Che, H., Qin, Y., Yang, F., Meng, S.-y., Li, X.-g., Bai, Y.-l. and Wang, L.-h. (2018). *Coriolus versicolor* aqueous extract ameliorates insulin resistance with PI3K/Akt and p38 MAPK signaling pathways involved in diabetic skeletal muscle. *Phytotherapy Research* 32, 551-560.
- [13] Muthukumaran, P., Thiyagarajan, G., Arun Babu, R. and Lakshmi, B. S. (2018). Raffinose from *Costus speciosus* attenuates lipid synthesis through modulation of PPARs/SREBP1c and improves insulin sensitivity through PI3K/AKT. *Chem Biol Interact* 284, 80-89.
- [14] Pemberton, J. G., Stafford, J. L., Yu, Y. and Chang, J. P. (2011). Differential involvement of phosphoinositide 3-kinase in gonadotrophin-releasing hormone actions in gonadotrophs and somatotrophs of goldfish, *Carassius auratus*. *J Neuroendocrinol* 23, 660-74.
- [15] Oak, J. S. and Fruman, D. A. (2007). Role of phosphoinositide 3-kinase signaling in autoimmunity. *Autoimmunity* 40, 433-41.
- [16] Qiao, X., Li, R., Song, W., Miao, W. J., Liu, J., Chen, H. B., Guo, D. A. and Ye, M. (2016). A targeted strategy to analyze untargeted mass spectral data: Rapid chemical profiling of *Scutellaria baicalensis* using ultra-high performance liquid chromatography coupled with hybrid quadrupole orbitrap mass spectrometry and key ion filtering. *J Chromatogr A* 1441, 83-95.
- [17] Zhang, Q. et al. (2017). Antimycobacterial and Anti-inflammatory Mechanisms of Baicalin via Induced Autophagy in Macrophages Infected with *Mycobacterium tuberculosis*. *Front Microbiol* 8, 2142.
- [18] Dai, J., Chen, L., Qiu, Y. M., Li, S. Q., Xiong, W. H., Yin, Y. H., Jia, F. and Jiang, J. Y. (2013). Activations of GABAergic signaling, HSP70 and MAPK cascades are involved in baicalin's neuroprotection against gerbil global ischemia/reperfusion injury. *Brain Res Bull* 90, 1-9.
- [19] Li, H. B. and Chen, F. (2005). Isolation and purification of baicalein, wogonin and oroxylin A from the medicinal plant *Scutellaria baicalensis* by high-speed counter-current chromatography. *J Chromatogr A* 1074, 107-10.
- [20] Guo, M. et al. (2013). Baicalin plays an anti-inflammatory role through reducing nuclear factor-kappaB and p38 phosphorylation in *S. aureus*-induced mastitis. *Int Immunopharmacol* 16, 125-30.

- Accepted Article
- [21] Fang, P., Yu, M., Zhang, L., Wan, D., Shi, M., Zhu, Y., Bo, P. and Zhang, Z. (2017). Baicalin against obesity and insulin resistance through activation of AKT/AS160/GLUT4 pathway. *Mol Cell Endocrinol* 448, 77-86.
- [22] Dai, J. et al. (2018). Chemoproteomics reveals baicalin activates hepatic CPT1 to ameliorate diet-induced obesity and hepatic steatosis. *Proc Natl Acad Sci U S A* 115, E5896-E5905.
- [23] Xi, Y. L. et al. (2016). Baicalin attenuates high fat diet-induced insulin resistance and ectopic fat storage in skeletal muscle, through modulating the protein kinase B/Glycogen synthase kinase 3 beta pathway. *Chin J Nat Med* 14, 48-55.
- [24] Ma, X., Zhang, Y., Wang, Z., Shen, Y., Zhang, M., Nie, Q., Hou, Y. and Bai, G. (2017). Ursolic Acid, a Natural Nutraceutical Agent, Targets Caspase3 and Alleviates Inflammation-Associated Downstream Signal Transduction. *Mol Nutr Food Res* 61, 1700332.
- [25] Saltiel, A. R. and Kahn, C. R. (2001). Insulin signalling and the regulation of glucose and lipid metabolism. *Nature* 414, 799-806.
- [26] Schultze, S. M., Hemmings, B. A., Niessen, M. and Tschopp, O. (2012). PI3K/AKT, MAPK and AMPK signalling: protein kinases in glucose homeostasis. *Expert Rev Mol Med* 14, e1.
- [27] Wang, T. et al. (2017). Baicalin and its metabolites suppresses gluconeogenesis through activation of AMPK or AKT in insulin resistant HepG-2 cells. *Eur J Med Chem* 141, 92-100.
- [28] Jo, H. et al. (2012). Small molecule-induced cytosolic activation of protein kinase Akt rescues ischemia-elicited neuronal death. *Proc Natl Acad Sci U S A* 109, 10581-6.
- [29] Meuillet, E. J. et al. (2010). Molecular pharmacology and antitumor activity of PHT-427, a novel Akt/phosphatidylinositide-dependent protein kinase 1 pleckstrin homology domain inhibitor. *Mol Cancer Ther* 9, 706-17.
- [30] Grimshaw, K. M. et al. (2010). AT7867 is a potent and oral inhibitor of AKT and p70 S6 kinase that induces pharmacodynamic changes and inhibits human tumor xenograft growth. *Mol Cancer Ther* 9, 1100-10.
- [31] Lindsley, C. W. et al. (2005). Allosteric Akt (PKB) inhibitors: discovery and SAR of isozyme selective inhibitors. *Bioorg Med Chem Lett* 15, 761-4.

- [32] Thomas, C. C., Deak, M., Alessi, D. R. and van Aalten, D. M. (2002). High-resolution structure of the pleckstrin homology domain of protein kinase b/akt bound to phosphatidylinositol (3,4,5)-trisphosphate. *Curr Biol* 12, 1256-62.
- [33] Chan, T. O. et al. (2015). Akt kinase C-terminal modifications control activation loop dephosphorylation and enhance insulin response. *Biochem J* 471, 37-51.
- [34] Kang, M. J. et al. (2014). Role of metabolism by intestinal microbiota in pharmacokinetics of oral baicalin. *Arch Pharm Res* 37, 371-8.
- [35] Zhang, L., Lin, G. and Zuo, Z. (2007). Involvement of UDP-glucuronosyl transferases in the extensive liver and intestinal first-pass metabolism of flavonoid baicalein. *Pharm Res* 24, 81-9.
- [36] Cross, D. A., Alessi, D. R., Cohen, P., Andjelkovich, M. and Hemmings, B. A. (1995). Inhibition of glycogen synthase kinase-3 by insulin mediated by protein kinase B. *Nature* 378, 785-9.
- [37] Ruan, X., Chen, T., Wang, X. and Li, Y. (2017). Suxiao Jiuxin Pill protects cardiomyocytes against mitochondrial injury and alters gene expression during ischemic injury. *Exp Ther Med* 14, 3523-3532.
- [38] Martins Pecanha, F. L., Dos Santos, R. S. and da-Silva, W. S. (2017). Thyroid states regulate subcellular glucose phosphorylation activity in male mice. *Endocr Connect* 6, 311-322.
- [39] Sakai, G. et al. (2017). Effects of the Activation of Three Major Hepatic Akt Substrates on Glucose Metabolism in Male Mice. *Endocrinology* 158, 2659-2671.
- [40] Andjelkovic, M. et al. (1997). Role of translocation in the activation and function of protein kinase B. *J Biol Chem* 272, 31515-24.
- [41] Stokoe, D. et al. (1997). Dual role of phosphatidylinositol-3,4,5-trisphosphate in the activation of protein kinase B. *Science* 277, 567-70.
- [42] Calleja, V., Laguerre, M., Parker, P. J. and Larjani, B. (2009). Role of a novel PH-kinase domain interface in PKB/Akt regulation: structural mechanism for allosteric inhibition. *PLoS Biol* 7, e17.
- [43] Khor, T. O., Gul, Y. A., Ithnin, H. and Seow, H. F. (2004). Positive correlation between overexpression of phospho-BAD with phosphorylated Akt at serine 473 but not threonine 308 in colorectal carcinoma. *Cancer Lett* 210, 139-50.

Author Contributions

G. B. and Y. H. designed the study; Y. Z. performed experiments, acquired and analyzed data, and drafted and edited the manuscript; F. S. synthesized baicalin probe; M. Z. performed Co-localization; X. M. performed molecule dynamic simulation and docking; Y. Z. performed SDS-PAGE and Western blotting for target confirmation. Y. Z., F. S., and X. M. assisted with experiments. G. B., Y. H., and S. Y. contributed to data discussion and review of the manuscript.

Acknowledgements

This work was supported by grants from the National Natural Science Foundation of China (Grant Numbers 81430095, 81473403, 81673616) and the International Cooperation and Exchange of the National Natural Science Foundation of China (Grant Number 81761168039)

Supporting information

Additional Supporting Information may be found online in the supporting information tab for this article:

Table S1. The top 30 target proteins (based on the fit value) predicted by PharmMapper

Table S2. The top five pathways (based on the q value) were selected by String 10.5

Figure S1. Synthetic route for the alkynyl-modified baicalin probe. Reagents and conditions: (a) Di-succinimidyl carbonate, pyridine; (b) DIEA, propargylamine.

Figure S2. The NMR data for the alkynyl-modified baicalin probe. (a) ^1H NMR spectrum of alkynyl-modified baicalin probe (400 MHz, DMSO-d₆) and (b) ^{13}C NMR spectrum of alkynyl-modified baicalin probe (100 MHz, DMSO-d₆).

Figure S3. (-)-HR-ESI-MS spectrum of the alkynyl-modified baicalin probe, as shown in Figure S3.

Figure S4. Synthetic route for the baicalin-modified functionalized MMs.

Reagents and conditions: (a) NH_2 -MMs, borate buffer, DMSO; (b) CuSO_4 , VC, methanol; (c) DTT, methanol.

Figure S5. UPLC/Q-TOF-MS/MS analysis of the solution of baicalin-modified functionalized MMs after DTT reduction.

Figure S6. The effect of baicalin and the alkynyl-modified baicalin probe on cell viability in the HepG 2 cells

Figure legends

Figure 1. Alkynyl-modified baicalin probe and MMs were used to obtain and verify the target protein from the cells

(A) Synthesis of the alkynyl-modified baicalin probe, preparation of the baicalin-modified functionalized MMs and the process for capturing and releasing the target protein. (B) Lane 1 shows the HepG-2 lysate, as a loading control, Lane 2 shows the lysate captured by the azide-modified MMs, as a negative control, and Lane 3 shows the lysate captured by the baicalin probe. The markers indicate the molecular weights. The concentrations of all the protein samples were adjusted to equal amounts before the capture and were adjusted to the same volume after the capture for the SDS-PAGE and western blot analyses. (C) Prediction of the targets of baicalin by using PharmMapper and the analysis of the interaction and signaling on the potential target proteins by String10.5.

Figure 2. Colocalization of the target protein and baicalin

(A) Synthesis of the fluorescent click product. (B) Analysis of the colocalization of the alkynyl-baicalin probe and the AKT protein using fluorescence confocal microscopy. The untreated group showed little fluorescence, but for the baicalin probe, obvious fluorescence was observed in the cytoplasm (green). The Alexa Fluor 594 staining for AKT (red) was observed in the cytoplasm and membrane and was partially colocalized with alkynyl-baicalin (yellow), as indicated by the arrows.

Figure 3. Baicalin binds to the AKT-PH domain and hampers AKT membrane translocation

(A) Competition tests of SC79, PHT-427, AT7867 and AKT inhibitor VIII with the baicalin probe against enriched AKT by functionalized MMs. Bands of AKT were detected by a western blot. Con, fished proteins by only azide-modified MMs; DTT, released proteins by DTT from the baicalin-modified MMs. The samples were replaced from the baicalin-modified MMs by treating with the same dose SC79, PHT-427, AT7867 and AKT inhibitor VIII,

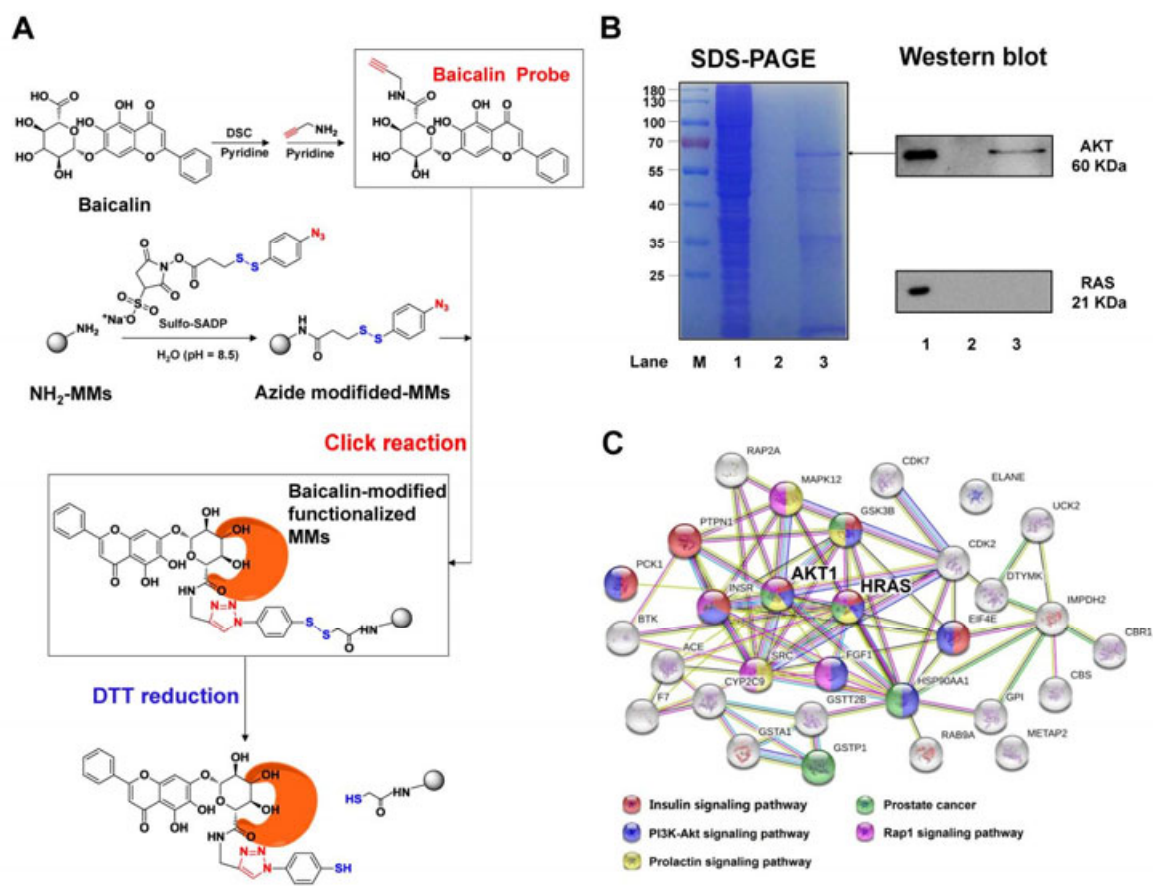
Accepted Article

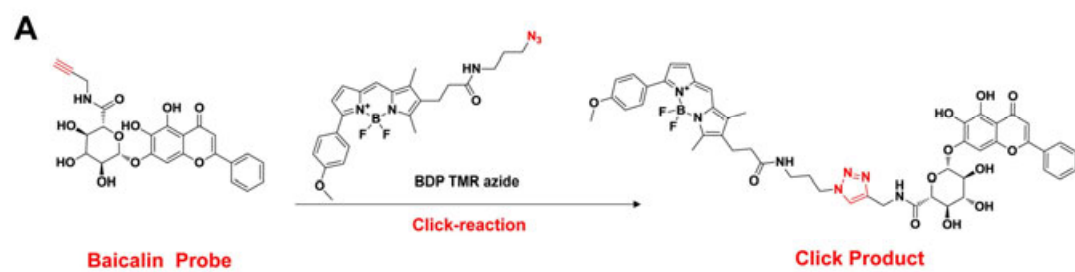
respectively. The histogram presents the relative intensity of the AKT bands. Each bar represents the mean \pm SD. *** $p < 0.001$ vs. Con group ($n = 3$). (B) Molecular docking analysis of SC79 and baicalin, and the mode of 4IP binding to the AKT-PH domain, as a comparison. The left is the AKT 3D surface form, shown as Pymol, and the right is the 2D interaction map, shown as Moe. A detailed docking model for the three ligands showed that R25 and N53 are the coincidences located in the AKT-PH domain. (C) Representative images show that the membrane translocation of AKT-PH with and without baicalin or baicalein treatment. The histogram presents the relative fluorescence of AKT^{PH}-GFP on the HEK 293T membrane. Each bar represents the mean \pm SD. ### $p < 0.001$ vs R25C; *** $p < 0.001$ and ** $p < 0.01$ vs R25 ($n = 10$).

Figure 4. Baicalin affects the activity of AKT and GSK3 β by acting on the phosphorylation of AKT itself and its downstream signaling, improving glucose metabolism

(A) Western blots showing the phosphorylation levels of the AKT upstream and downstream effectors of PDK1, AKT (Thr308 and Ser473) and GSK3 β , which were treated with different doses of baicalin. GAPDH expression was used as an internal control for normalization. Each bar represents the mean \pm SD. * $p < 0.05$ and ** $p < 0.01$ vs Con group ($n = 3$). (B, C) The enzymatic activity of AKT and GSK3 β in the HepG-2 cells lysate after treatments with different concentrations of baicalin. SC79 and LiCl was used as positive controls for AKT and GSK3 β activity detection, respectively. Each bar represents the mean \pm SD. * $p < 0.05$, ** $p < 0.01$ and *** $p < 0.001$ vs Con group ($n = 3$). (D) Effect of baicalin with different concentrations on glucose consumption in the insulin-treated HepG-2 cells. Met served as a positive control. Each bar represents the mean \pm SD. ## $p < 0.01$ vs Con group; * $p < 0.05$ and ** $p < 0.01$ vs Mod group ($n = 6$).

Figure 5. Baicalin targets the AKT-PH domain, activates AKT/GSK3 β phosphorylation and improves glucose metabolism





B

Alk-Baicalin(10uM)	-	+
BDP TMR azide (10uM)	+	+
AKT	+	+
FSA	+	+

